

# Primary Kinetic Isotope Effects in Hydride Transfer: Experimental Studies of Intramolecular Hydride Migration and *ab initio* Molecular Orbital Calculations of Model Systems

Ian H. Hillier,\* Stephen Smith, Stephen C. Mason, Stephen N. Whittleton, C. Ian F. Watt,\* and Julie Willis

Chemistry Department, University of Manchester, Manchester M13 9PL

Measurements of the primary kinetic hydrogen isotope effects for the intramolecular migration of hydride accompanying the rearrangements of (i) hydroxy-ketones involving 1,4-migration of hydride between ketonic carbonyl groups and (ii) phenylglyoxal hydrates to their corresponding mandelic acids are described. The results are discussed using *ab initio* MO calculations of model systems, with a variety of basis sets. The value of such model calculations is demonstrated.

Formal transfers of hydride between electrophilic carbon are common in organic chemistry, occurring, for example, in biological redox processes involving the nicotinamide cofactors,<sup>1</sup> and industrially important reactions involving inter- and intramolecular transfer of hydride between cationic centres in hydrocarbons.<sup>2</sup> Despite the familiarity of the overall reaction sequences, relatively little is known of the actual transfer step, particularly when the situation is compared with that for proton transfers. For the experimentalist, there are difficulties in characterising hydride-transfer transition states since they often occur centrally as a low activation energy step in a complex reaction sequence. From the theoretical standpoint the complexity of the systems studied experimentally means that rarely can theoretical treatments, other than semiempirical ones, be utilised to investigate the nature of the transition state.

The potential of the primary kinetic isotope effect (k.i.e.) associated with the migrating hydrogen in characterising the transition state is acknowledged,<sup>3</sup> with comparison being made between experimental values and those calculated with various assumptions of transition-state geometry and force constant behaviour.<sup>4</sup> However, the use of higher levels of theory for comparison between theory and experiment is usually prohibited due to the size of the systems studied experimentally, although *ab initio* calculations on small model systems have been reported.<sup>5</sup> In order to provide experimental data of k.i.e.s for well defined systems with the minimum of complexity we are studying two classes of intramolecular hydride migrations (see Figure 1): (i) rearrangements of hydroxy-ketones involving 1,4-migration of hydride between ketonic carbonyl groups, and (ii) rearrangements of phenyl- and substituted phenyl-glyoxal hydrates to their corresponding mandelic acids, which are believed to involve a 1,2-hydride shift. The smaller examples of such systems can be treated using *ab initio* molecular orbital (MO) methods to locate the stationary points on the potential energy surface for hydride transfer, and following the calculation of the associated harmonic frequencies estimates of the k.i.e. can be obtained.

However, due to the size of these systems only minimal basis set calculations at the single determinantal level can be carried out in reasonable amounts of computer time. For this reason it is of value to investigate predictions of transition-state structure, energetics, and associated k.i.e.s for smaller model systems, using various levels of approximation to obtain information on the reliability of the more approximate calculations carried out on the experimentally investigated molecules.

To model these two classes of reaction mentioned above we chose, respectively, the degenerate model reactions (i) and (ii)

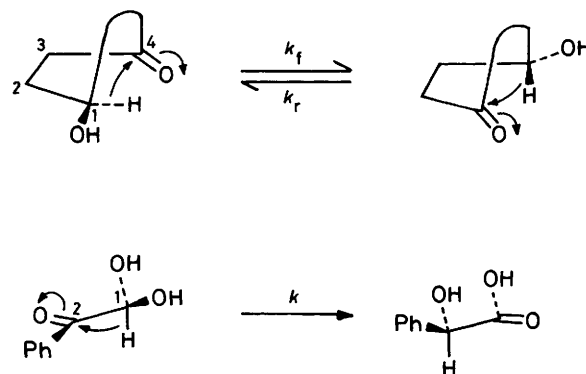
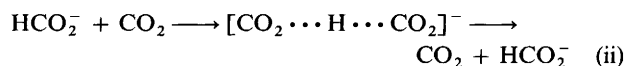
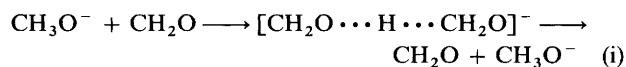


Figure 1. Rearrangements involving 1,4- or 1,2-hydride shifts



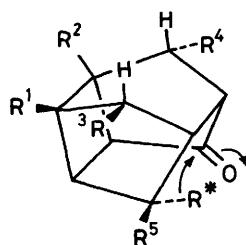
and herein report *ab initio* MO calculations of these systems leading to values for the k.i.e. for these reactions.

Direct comparison of the results of our model calculations with experiment is not possible. Thus, while solution-phase reactions in which methoxide or formate donate hydride to electrophilic carbon are well known, kinetic isotope effect measurements are rare. Swain,<sup>6</sup> for example, has measured  $k(\text{CH}_3)/k(\text{CD}_3) = 2.2$  for base-catalysed reduction of benzaldehyde by methanol. For reductions of substituted triarylmethyl carbonium ions by formate, a spread of values,  $1.8 < k_{\text{H}}/k_{\text{D}} < 3.2$ , dependent on  $\text{p}K_{\text{a}}$  of the cation have been reported.<sup>7</sup> In the closely related formate reduction of the *N*-methylacridinium cation,  $k_{\text{H}}/k_{\text{D}} = 2.74$  at 50 °C.<sup>8</sup> These are all relatively small primary effects but these reactions are so complex that they can hardly be taken as a reasonable test of the calculations. Indeed, there has been extensive discussion on whether the rate-determining step in the reductions of the cations involves delivery of hydride rather than sigmatropic rearrangement of adducts between cation and donor.<sup>9</sup> The simple symmetrical processes for which our calculations have been undertaken have not been experimentally observed in solution, but recently, Sheldon and Bowie have observed the gas-phase reactions.<sup>10</sup> Unfortunately,

no gas-phase k.i.e. measurements are yet available for direct comparison with calculation.

Experimental difficulties in the examination of the model reactions in solution arise mainly from competing reactions in which the oxyanions behave as nucleophiles or bases, rather than hydride donors. We have therefore examined simple intramolecular variants which retain the feature that the hydride donor is carbon-bearing anionic oxygen and the acceptor is carbonyl carbon, but which exclude complicating reactions by the arrangement of these functional groups within the molecular framework.<sup>11</sup> Primary kinetic hydrogen isotope effect measurements for three such rearrangements are presented here. In addition we report a minimal basis calculation for the intramolecular hydride transfer in a hydroxy-ketone, to provide a direct theoretical comparison with the experimentally determined k.i.e.s which we present in this paper.

**Measurements of Kinetic Isotope Effect.**—The unsymmetrically methylated polycyclic hydroxy-ketones (**1a** and **b**) were prepared by reduction and photoclosure of the isoprene-benzo-



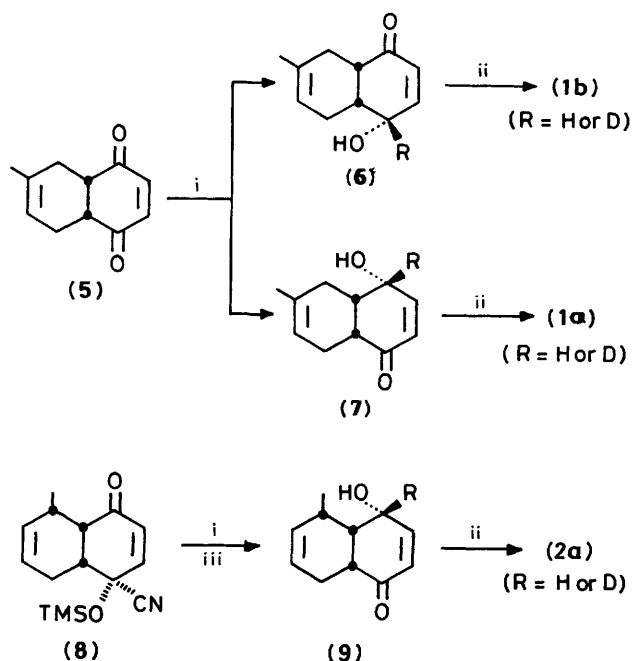
(R = H or D)

- (1a)  $R^1 = \text{Me}; R^2, R^3, R^4, R^5 = \text{OH}$   
 (1b)  $R^2 = \text{Me}; R^1, R^3, R^4, R^5 = \text{OH}$   
 (2a)  $R^3 = \text{Me}; R^1, R^2, R^4, R^5 = \text{OH}$   
 (2b)  $R^4 = \text{Me}; R^1, R^2, R^3, R^5 = \text{OH}$   
 (3)  $R^1, R^2 = \text{H}; R^3, R^4 = \text{Me}; R^5 = \text{OH}$   
 (4)  $R^1, R^2, R^3, R^4 = \text{H}; R^5 = \text{O}^-$

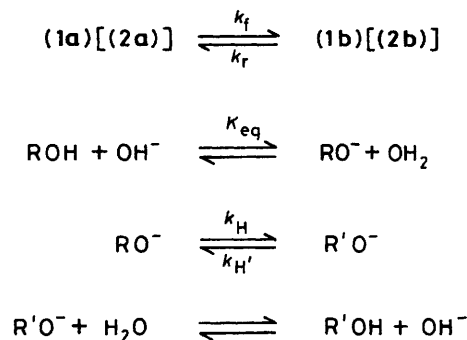
quinone Diels–Alder adduct (**5**) as shown in Scheme 1. The well precedented sequence<sup>12</sup> leads logically to the indicated mixture of (**1a** and **b**) which was separated chromatographically.

Both products isolated have spectroscopic and analytical properties in full accord with the indicated structures, and the isomers could be distinguished by their <sup>1</sup>H n.m.r. spectra. In both isomers, the *exo*-hydrogen on the C-10 bridges ( $R^4$  position) lie in the anisotropic shielding cone of the carbonyl and give the highest field signals (*ca.*  $\delta$  1.0), well clear of the remainder of the spectrum. In the case of (**1a**) this signal is a doublet of triplets, *J* 14.0 and 3.5 Hz, showing geminal and vicinal coupling to two adjacent hydrogens. In the case of (**1b**), the signal is a doublet of doublets, *J* 12.0 and 2.5 Hz, also showing geminal and vicinal coupling to only a single adjacent hydrogen. The deuteriated compounds were prepared by use of borodeuteride rather than borohydride in the sequence.

Compounds (**1a** and **b**) could be equilibrated in aqueous basic dioxane at near room temperatures, and reactions could be monitored by conventional sampling and g.l.c. analysis of the trimethylsilyl ethers. At equilibrium, the major component of the mixture is (**1b**),  $K_e$  1.84 ( $\pm$  0.03) at 25 °C. Reactions were cleanly first order in hydroxy-ketone and in catalysing base, and no dependence of rate on buffer concentration could be detected.<sup>13</sup> With deuteriated substrates, rearrangement occurred without loss of deuterium content. Taken together, the data



Scheme 1. Reagents: i, NaBH<sub>4</sub> or NaBD<sub>4</sub>; ii, *h* $\nu$  in PhH; iii, NaF in aqueous THF



$$(k_f + k_r) = \frac{K_a[OH^-]}{K_w} (k_H + k_{H'})$$

$$K_a = \frac{[RO^-][H^+]}{[ROH]} = \frac{[R'O^-][H^+]}{[R'OH]}$$

Scheme 2.

are consistent with Scheme 2 involving rate-limiting hydride shift (governed by  $k_H$  or  $k_{H'}$ ) within the alkoxide anions. The relationship between the experimentally determined pseudo-first-order rate constants and those in Scheme 2 is shown, and it is clear that the kinetic isotope effects quoted will contain a contribution from a  $\beta$ -D equilibrium isotope effect on the acidity ( $K_a$ ) of the alcohols. We have no experimental data on these compounds, but acidity measurements on methanol and [<sup>2</sup>H<sub>3</sub>]methanol suggest that  $K_{BH}/K_{BD}$  may be *ca.* 1.3.<sup>14</sup>

A second unsymmetrically methylated hydroxy-ketone (**2a**) was prepared from the Diels–Alder adduct of piperylene-benzoquinone derivative (**8**)<sup>15</sup> as shown in Scheme 1. This sequence leads cleanly to a single hydroxy-ketone, which was converted completely into an isomeric hydroxy-ketone by action of

**Table 1.** Rate and kinetic hydrogen isotopes data for base-catalysed equilibrations of hydroxy-ketones (**1a** and **b**) and (**2a** and **b**)

Equilibrium	<i>T</i> /°C	pH	$10^4 (k_1 + k_{-1})_{\text{H}}/\text{s}^{-1}$	$(k_{\text{f}} + k_{\text{r}})_{\text{H}}/(k_{\text{f}} + k_{\text{r}})_{\text{D}}$
( <b>1a</b> ) + ( <b>1b</b> )	17.2	14.3	4.01 (±0.02)	3.71 (±0.03)
( <b>1a</b> ) + ( <b>1b</b> )	27.3	13.7	1.10 (±0.01)	3.56 (±0.07)
( <b>1a</b> ) + ( <b>1b</b> )	40.0	13.7	4.55 (±0.04)	3.37 (±0.04)
( <b>1a</b> ) + ( <b>1b</b> )	54.9	13.7	22.1 (±0.10)	3.27 (±0.04)
( <b>1a</b> ) + ( <b>1b</b> )	69.7	12.3	3.63 (±0.07)	3.10 (±0.08)
( <b>2a</b> ) + ( <b>2b</b> )	14.8	12.94	10.3 (±0.2)	3.64 (±0.07)
( <b>2a</b> ) + ( <b>2b</b> )	25.0	12.94	33.4 (±0.1)	3.40 (±0.21)
( <b>2a</b> ) + ( <b>2b</b> )	40.0	12.31	13.4 (±0.5)	2.92 (±0.14)
( <b>2a</b> ) + ( <b>2b</b> )	49.9	12.31	34.4 (±0.3)	2.71 (±0.11)
( <b>2a</b> ) + ( <b>2b</b> )	69.7	11.31	43.6 (±0.1)	2.56 (±0.09)

<sup>a</sup> These are the mean and standard deviation of at least three runs in the case of  $(k_1 + k_{-1})_{\text{H}}$  or three pairwise determinations in the case of the k.i.e.

aqueous base. In accord with spectroscopic and analytical data, and the fact that oxidation of (**2a**) and its isomer yielded the same dione, the isomer is assigned structure (**2b**), being formed from (**2a**) by the same hydride shift mechanism outlined above. The conversions of (**2a**) into (**2b**) were similarly well behaved, and could be monitored by sampling and analysis of the tri-fluoroacetates of the hydroxy-ketones.

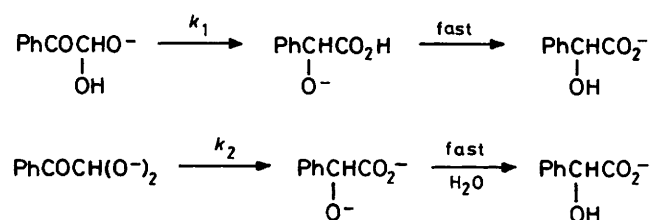
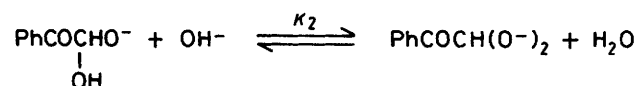
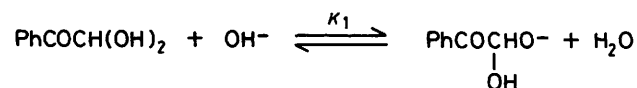
Pseudo-first-order rate constants and hydrogen k.i.e.s determined at a variety of temperatures are presented in Table 1. Equilibrium i.e.s were also measured for the reaction of (**1a**), but in all cases these were unity within experimental uncertainty. The sampling techniques that we have used work most conveniently for reaction half-lives between 15 min and 1 h, and to obtain kinetic isotope effects over a wide range of temperatures, solution pH values were adjusted to maintain half-lives in this range.

The symmetrically methylated hydroxy-ketone (**3**) and its deuteriated isotopomer were prepared by literature methods.<sup>16</sup> Rates of degenerate rearrangement of alkali-metal salts of this compound have been previously measured by dynamic <sup>1</sup>H n.m.r. methods. Hydride transfer between the oxygenated carbons exchanges chemical environments of the pendant methyls, and signals from these are well resolved and their behaviour may be subjected to total line-shape analysis.<sup>17</sup> Rates of rearrangement under these conditions are strongly dependent on cation, concentration, and presence of trace impurities, and it was extremely unlikely that conditions could be reproduced in separate measurement of rates for (**4**) and its isotopomer. Primary hydrogen k.i.e.s were thus determined by analysis of the spectra of a known *ca.* 1 : 1 mixture of the salts of deuteriated and undeuteriated materials in [<sup>2</sup>H<sub>6</sub>]dimethyl sulphoxide. The line shape in the region of the methyl signals was calculated, summing the contributions from the known ratio of the components and fitted to the experimental spectra using a standard non-linear least-squares fitting method,<sup>18</sup> with the  $k_{\text{H}}/k_{\text{D}}$  ratio as an additional parameter to be determined. Trials with synthetic spectra showed, not surprisingly, that the total line shapes would be most sensitive to the k.i.e. with rates between those for coalescence of peaks from the individual components. By adjustment of concentrations, k.i.e.s have been measured at a range of temperatures, and the data are given in Table 2.

Finally, we report k.i.e. data for the base-induced rearrangement of phenylglyoxal hydrate to mandelate. Use of <sup>13</sup>C-labelled substrates has shown this to involve migration of the formyl hydrogen to the adjacent carbonyl carbon.<sup>19</sup> Kinetic studies are consistent with Scheme 3<sup>20</sup> in which the hydrogen motion is hydride shift in either the mono- or di-anion of the hydrate. The resultant rate law is complex (see Scheme 3), but

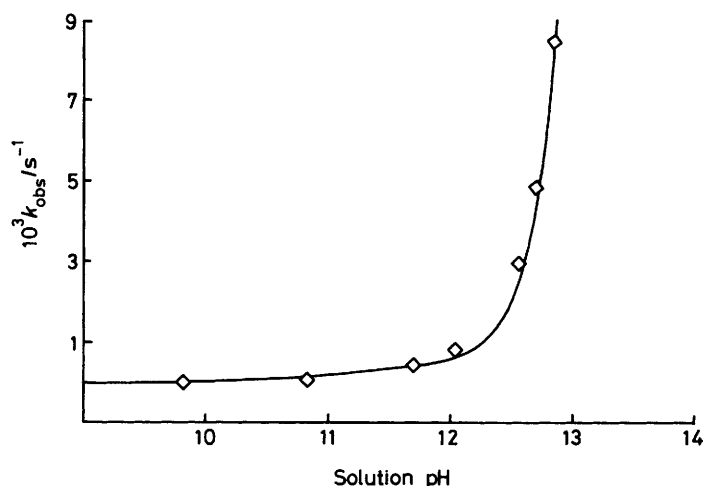
**Table 2.** Kinetic hydrogen isotope effects for rearrangements of sodium salts of (**3a**) in [<sup>2</sup>H<sub>6</sub>]dimethyl sulphoxide solution

Mean temperature (°C)	Concentration (M)	Isotope ratio [H]/[D]	$k_{\text{H}}/k_{\text{D}}$
32	0.03	1.200	2.76 (±0.23)
63	0.30	1.200	2.52 (±0.19)
86	2.36	1.200	2.36 (±0.19)



$$k_{\text{obs}} = \frac{\kappa_1 [\text{OH}^-]}{1 + \kappa_1 [\text{OH}^-]} (k_1 + k_2 \kappa_2 [\text{OH}^-])$$

Scheme 3.

**Figure 2.** pH Dependence of the pseudo-first-order rate constants for rearrangement of phenylglyoxal hydrate to mandelate in aqueous solution at 25.6 °C and ionic strength 0.1M

the shift within the dianion is expected to be orders of magnitude faster than that within the monoanion, so that its contribution dominates, except at very low pH values. A plot of pseudo-first-order rate constants against pH is shown in Figure 2. The solid line represents rates calculated using the rate law derived from the scheme with  $k_1$  0.0005,  $k_2$  0.4 s<sup>-1</sup>. For the first ionisation,  $\text{p}K_{\text{a}1}$  11.20 has been measured. The second constant is not experimentally accessible, but typically first and second

ionisations of stronger acids of the form  $R_2X(OH)_2$  where X is S or P differ by *ca.* 5  $pK_a$  units<sup>21</sup> and we have set  $pK_{a2}$  16.2 in calculating the line.

Vander Jagt<sup>22</sup> has reported a primary hydrogen k.i.e.  $k_H/k_D$  5.0 (pH 12; 25 °C), a value which seems to us to be unusually large for this type of reaction. We have redetermined the kinetic isotope effect associated with migrating hydride, also at pH 12, at a range of temperatures. At pH 12, phenylglyoxal hydrate exists > 99% as its monanion. The experimental kinetic isotope effects therefore apply to conversion of this ion into mandelate, and will contain a contribution from  $\beta$ -D equilibrium isotope effect, in this case, on the second ionisation. The data are collected in Table 3, and our range of measurements are notably lower than those of Vander Jagt. We can offer no reason for the discrepancy between our data and the earlier measurements.

**Computational Methods.**—Calculations were carried out using the standard basis sets of Pople and his co-workers<sup>23</sup> using where necessary the polarisation functions of Ahlrichs and Taylor.<sup>24</sup> Stationary points (minima and saddle points) on the potential energy surface of the reactions studied were located by the use of analytic gradients of the energy as implemented in the program GAMESS,<sup>25</sup> and harmonic frequencies were calculated using analytic second derivatives of the energy using the program CADPAC.<sup>26</sup> Correlation effects were included by means of configuration interaction (CI) calculations, using the ATMOL system of programs.<sup>27</sup> The CI expansion included single and double excitations from all filled valence to all virtual orbitals.

The semi-classical k.i.e. values were computed at a number of temperatures within the ideal gas, rigid rotor, harmonic oscillator approximation, with corrections for quantum mechanical tunnelling using Bell's model approximation.<sup>28</sup> Here, the tunnel correction ( $Q_t$ ) to the semi-classical expression for the reaction rate is given as (iii) in which  $u^+ = hv^+/kT$  and  $y = \exp(-2\pi E/$

$$Q_t = \frac{u^+/2}{\sin(u^+/2)} - u^+ y^{-u^+/2\pi} [y/(2\pi - u^+) - y^2/(4\pi - u^+) + y^3/(6\pi - u^+) \dots] \quad (\text{iii})$$

**Table 3.** Pseudo-first-order rate constants and kinetic hydrogen isotope effects for rearrangement of phenylglyoxal hydrate to mandelate in buffered aqueous solution at pH 12

$T/^\circ\text{C}$	$10^4 k_H/s^{-1}$	$k_H/k_D$
16.9	1.95 ( $\pm 0.02$ )	3.75 ( $\pm 0.02$ )
31.8	10.1 ( $\pm 0.2$ )	3.13 ( $\pm 0.02$ )
39.2	20.9 ( $\pm 0.7$ )	2.74 ( $\pm 0.04$ )
57.7	66.1 ( $\pm 1.5$ )	2.59 ( $\pm 0.01$ )

<sup>a</sup> These are mean and standard deviations of three or more runs in the case of  $k_H$  or three pairwise determinations in the case of  $k_H/k_D$ .

$u^+kT$ ) with  $v^+$  being the barrier frequency, and  $E$  the barrier height. These latter two quantities are determined from our calculations of the reactants and transition state. The harmonic frequencies used for reactions (i) and (ii) were those calculated, uniformly scaled to give the best fit to the experimental frequencies for formaldehyde and carbon dioxide respectively.<sup>29</sup> Scale factors in the range 0.81–0.96 resulted from such a procedure.

**Computational Results.**—(1)  $\text{CH}_3\text{O}^- + \text{H}_2\text{CO}$ . The geometries and energies of the two transition states, the *cis*-(10) and *trans*-(11) structures (Figure 3), are given in Table 4. Where there is overlap with the calculations of Wu and Houk,<sup>30</sup> excellent agreement is found. For all three basis sets used (STO-3G, 3-21G, 6-31G\*\*) the *trans* structure (11) is a true transition state with a single imaginary frequency, whilst the *cis* structure (10) has a second, small, imaginary frequency corresponding to rotation to the slightly more stable *trans* structure (11). As far as a model for the hydride migration within the hydroxy-ketones (1)–(4) is concerned, the calculations for the *cis* structure are most relevant. For this structure of  $C_{2v}$  symmetry, all basis sets predict a bent transition state with a  $\text{CHC}$  angle decreasing from 165 to 140° as the quality of the basis set improves. The quantities associated with the calculation of the k.i.e.s ( $k_H/k_D$ ) are summarised in Table 5. The barrier to the reaction increases substantially on improvement in the basis, but is drastically decreased upon the inclusion of correlation effects. The

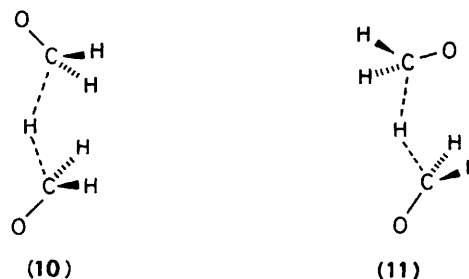


**Figure 3.**

**Table 5.** Calculated k.i.e.s (at 25 °C) for the *cis* transition state [ $\text{CH}_2\text{O} \cdots \text{H} \cdots \text{CH}_2\text{O}$ ]<sup>−</sup>

Basis	$v_H^+/\text{cm}^{-1}$	$v_D^+/\text{cm}^{-1}$	$(k_H/k_D)_s$	$Q_t^H/Q_t^D$	$k_H/k_D$
STO-3G	933i	785i	2.54	1.23	3.11
3-21G	1 308i	1 067i	2.86	2.24	6.40
6-31G**	1 416i	1 149i	3.03	3.69	11.15
[STO-3G	1 131i	956i	2.67	1.44	3.84] <sup>a</sup>

<sup>a</sup> This line refers to the transition state for the rearrangement of (4) (Figure 4).

**Table 4.** Geometries (Å and °) and energies<sup>a</sup> (kJ mol<sup>−1</sup>) of *cis*-(10) and *trans*-(11) transition states<sup>b</sup> [ $\text{CH}_2\text{O} \cdots \text{H} \cdots \text{CH}_2\text{O}$ ]<sup>−</sup>

Basis	Bond length		Bond angle		$E$
	CO	CH	$\widehat{\text{CHC}}$	$\widehat{\text{OCH}}$	
STO-3G	1.273 (1.276)	1.374 (1.368)	165.0 (180.0)	114.9 (113.8)	27.5 (21.9)
3-21G <sup>c</sup>	1.261 (1.251, 1.278)	1.464 (1.552, 1.346)	151.5 (133.8)	118.1 (109.5, 117.7)	32.8 (12.3)
6-31G** <sup>c</sup>	1.232 (1.227, 1.246)	1.447 (1.493, 1.354)	140.4 (137.1)	115.7 (111.7, 115.6)	48.1 (29.2)
6-31G** + SDCI//6-31G**					15.6 (−2.5)
[STO-3G	1.256	1.380	122.3		77.4] <sup>d</sup>

<sup>a</sup> The energies are given relative to  $\text{CH}_3\text{O}^- + \text{CH}_2\text{O}$ . <sup>b</sup> The parameters are given for the *cis*, followed by those for the *trans* structure in parentheses. <sup>c</sup> For the *trans* structure, the values in parentheses refer to the non-equivalent  $\text{H} \cdots \text{CO}$  groups. <sup>d</sup> This line refers to the transition state for the rearrangement of (4) (Figure 4).



imaginary frequency corresponding to hydride migration ( $\nu_{\text{H}}^+$ ,  $\nu_{\text{D}}^+$ ) also increases substantially upon basis set improvement, such increase being little affected by scaling.

For all basis sets, the semi-classical contribution to the k.i.e. ( $k_{\text{H}}/k_{\text{D}}$ )<sub>s</sub> is in the range 2.5–3.0. However, our calculated tunnel correction ( $Q_{\text{t}}^{\text{H}}/Q_{\text{t}}^{\text{D}}$ ) to the semi-classical k.i.e. is seen to be extremely dependent upon basis set, greatly increasing as the quality of the basis set is improved owing to the corresponding increase in the barrier height and frequency.

Turning now to our calculations of the hydroxy-ketone (4), which is close in structure to those measured experimentally, we show in Figure 4 the predicted transition state structure. A characterisation of the transition state by determination of the harmonic frequencies yielded a single imaginary frequency. The calculated frequencies were scaled by 0.83 and yielded the k.i.e.s shown in Table 6. Although the barrier is much larger than those calculated for the model reaction, due to the different reactant structures in the two cases, both the barrier frequencies and the contributions to the k.i.e. are very close to those for the model reaction calculated in an STO-3G basis, giving us some confidence that the model calculations are useful in understanding the more complex systems studied experimentally.

(2)  $\text{CO}_2 + \text{HCO}_2^-$ . Two transition state structures were studied with staggered (12) and eclipsed (13) oxygen atoms

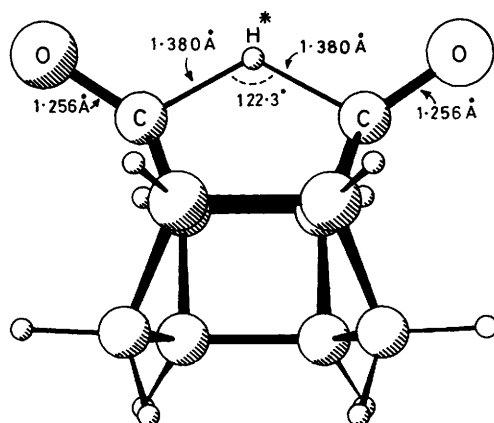


Figure 4. Details of the STO-3G-computed transition state for the rearrangement of (4)

Table 6. Calculated k.i.e.s for the rearrangement of (4)

$T/^\circ\text{C}$	$(k_{\text{H}}/k_{\text{D}})_s$	$Q_{\text{t}}^{\text{H}}/Q_{\text{t}}^{\text{D}}$	$k_{\text{H}}/k_{\text{D}}$
0	2.90	1.64	4.76
25	2.67	1.44	3.84
50	2.49	1.33	3.31
75	2.34	1.26	2.95

(Figure 5). The geometries and energies of these species are given in Table 7. At the STO-3G level, the staggered form was a true transition state, whilst the eclipsed had a second, very small imaginary frequency ( $14i \text{ cm}^{-1}$ ), with the former being of lower energy. At the 3-21G level, both structures were true transition states, with the eclipsed now being of lower energy. In the 6-31G\*\* basis, the eclipsed structure is of lower energy with a single imaginary frequency, whilst the staggered had two such frequencies. All structures yielded a linear CHC arrangement except for the eclipsed form in the 3-21G basis, where the angle is  $166^\circ$ . The values of the k.i.e. shown in Table 8 are for the eclipsed structures, since the trends are the same for both structures studied. These trends parallel those previously discussed for the  $\text{CH}_3\text{O}^- + \text{CH}_2\text{O}$  reaction. As the quality of the basis set is increased, the barrier rises, but is substantially reduced upon inclusion of correlation effects. There is a corresponding increase in the semi-classical contribution to the k.i.e. and, more markedly, in the tunnelling correction to the k.i.e. Here the increase in the tunnelling correction is substantially less than for the  $\text{CH}_3\text{O}^- + \text{CH}_2\text{O}$  reaction due to the greater heavy atom contribution to the vibrational mode having the imaginary frequency. This is reflected in a decrease in the ratio  $\nu_{\text{H}}^+/\nu_{\text{D}}^+$ . However, it is of interest that for both reactions the semi-classical k.i.e. is in the range 2.5–3.0, with greater variations in the tunnelling correction.

## Discussion

Calculations have been carried out in order to investigate the effect of basis set changes upon the structure, energetics, and k.i.e.s for two model reactions which are hoped to be relevant to a study of the two classes of intramolecular hydride shifts which

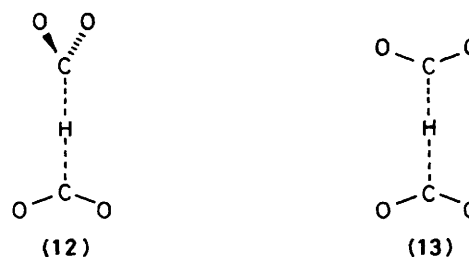


Figure 5.

Table 8. Calculated k.i.e.s (at  $25^\circ\text{C}$ ) for the eclipsed transition state  $[\text{CO}_2 \cdots \text{H} \cdots \text{CO}_2]^-$

Basis	$\nu_{\text{H}}^+/\text{cm}^{-1}$	$\nu_{\text{D}}^+/\text{cm}^{-1}$	$(k_{\text{H}}/k_{\text{D}})_s$	$Q_{\text{t}}^{\text{H}}/Q_{\text{t}}^{\text{D}}$	$k_{\text{H}}/k_{\text{D}}$
STO-3G	456	421	2.55	1.03	2.63
3-21G	1 006	885	2.59	1.39	3.60
6-31G**	1 181	1 038	2.72	1.62	4.41

Table 7. Geometries ( $\text{\AA}$  and  $^\circ$ ) and energies<sup>a</sup> ( $\text{kJ mol}^{-1}$ ) of eclipsed (13) and staggered (12) transition states<sup>b</sup>  $[\text{CO}_2 \cdots \text{H} \cdots \text{CO}_2]^-$

Basis	Bond length		Bond angle		$E$
	CO	CH	CHC	OCH	
STO-3G	1.229 (1.229)	1.385 (1.386)	180.0 (180.0)	109.0 (109.0)	16.3 (13.4)
3-21G	1.202 (1.203)	1.379 (1.401)	166.4 (180.0)	107.8 (108.2)	56.6 (57.2)
6-31G**	1.181 (1.181)	1.389 (1.400)	180.0 (180.0)	107.3 (107.4)	86.5 (88.7)
6-31G** + SDCI//6-31G**					56.1 (59.9)

<sup>a</sup> The energies are given relative to  $\text{CO}_2 + \text{HCO}_2^-$ . <sup>b</sup> The parameters are given for the eclipsed, followed by those for the staggered structure in parentheses.

we have investigated experimentally. For these latter reactions only minimal basis set calculations are feasible in realistic amounts of computer time.

In view of the structural similarities, it is expected that the methoxide-formaldehyde system will quite closely model the hydroxy-ketone intramolecular rearrangement. Due to the structural differences between the model and experimental systems, the transferability of conclusions for the carbon dioxide-formate system to the phenylglyoxals must be viewed with more caution.

For the methoxide-formaldehyde reaction, a bent transition state is generally predicted, with the barrier predicted at the STO-3G level being closer to the CI value than that found for the larger basis sets. Hence, the barrier calculated for the rearrangement of (4) at the STO-3G level is probably not unreasonable. Indeed, this calculated barrier height, 77.7 kJ mol<sup>-1</sup>, compares very well with the Arrhenius activation energy of 85.8 (±0.8) kJ mol<sup>-1</sup> for the rearrangement of (1a). For (2a) the experimental value, 62.3 (±2.4) kJ mol<sup>-1</sup>, is rather low and is possibly accounted for by relief of the ground-state steric compression between the hydroxy group function and the pendant methyl group. Rearrangement of (3) is the closest approach we have to the 'gas phase' data of the calculation. The experimental estimate of the barrier (50.2 kJ mol<sup>-1</sup>) is again lower than the calculated value, which may be attributed to the presence of the pendant methyl groups in the experimental substrate. The values of the k.i.e.s calculated in a STO-3G basis for the model system, and for (4), are quite close, again showing the value of our model calculations. The calculations predict a relatively large (ca. 40%) contribution from quantum mechanical tunnelling, resulting in calculated k.i.e.s that are rather larger than experiment (Tables 1, 2, and 6). Agreement between theory and experiment is quite good if the tunnelling correction is removed. Certainly for the rearrangement of (3), the activation parameter ratios ( $A_H/A_D$  0.98;  $[\Delta E]_D^H$  2.6 kJ mol<sup>-1</sup>) are not consistent with extensive tunnelling.

Following our discussion of the hydroxy-ketones, we consider that for the model system, carbon dioxide-formate, the STO-3G values of the k.i.e. are probably the most useful. Here, the tunnelling contribution is smaller than for the methoxide-formaldehyde system resulting in a smaller net value for  $k_H/k_D$ , which is somewhat smaller than the experimental value (Table 3). However, in spite of the possible lack of realism of the system used to model the phenylglyoxals, it is of interest to note that the calculated k.i.e.s for both model systems are quite similar, as are the experimental values for the two classes of reactions studied herein.

## Experimental

<sup>1</sup>H N.m.r. spectra were recorded on either a Perkin-Elmer 90 MHz R32 or a Varian SC 300 MHz spectrometer. Unless otherwise stated, the solvent was deuteriochloroform with tetramethylsilane as internal reference. I.r. spectra were determined on a Pye-Unicam SP3-200 spectrophotometer, using 0.1 mm solution cells with carbon tetrachloride as solvent. Mass spectra were recorded on a Kratos MS 25 machine operating at 70 eV for electron impact ionisation. The g.l.c.-m.s. spectra were run on a Perkin-Elmer Sigma 3 g.l.c. machine in conjunction with the Kratos MS 25 instrument. For all chemical ionisation spectra, ammonia was the reagent used. U.v. spectra were recorded on a Pye-Unicam SP8-300 u.v.-visible spectrophotometer, with the cell block kept at constant temperature by Haake E3 thermostat bath. For g.l.c., a Carlo Erba Strumentazione machine with a 20 m OV-1 glass capillary column using hydrogen carrier gas and a flame ionisation detector was used in all cases. Merck G alumina was used for alumina columns, Merck Kieselgel 60 H silica for silica

columns, and Merck Kieselgel 60 PF254 silica for preparative t.l.c. For t.l.c., Merck precoated silica-backed plates with a 0.2 mm layer of Kieselgel 60 F254 were used. All microanalyses were carried out by the University of Manchester Microanalysis Laboratory under the direction of Mr. M. Hart. Dioxane and 2,2,2-trifluoroethanol were purified by literature methods.<sup>31</sup>

**Reductions of the Isoprene-Benzoquinone Adduct.**—A solution of the adduct (5)<sup>32</sup> (4.9 g) in methanol (150 ml) and water (2 ml) was stirred and ice-cooled in a conical flask. Sodium borohydride (0.27 g) was added in portions over 20 min, such that the temperature did not exceed 4 °C. After 1 h, acetic acid (2 ml) was added and the volume reduced under vacuum to ca. 50 ml. Ice-water (100 ml) was then added before extracting with ether (3 × 30 ml). The combined organic layers were dried (MgSO<sub>4</sub>) and evaporated to yield a dark oil (3.7 g), shown by g.l.c. to contain two components in nearly equal amounts. Chromatography on silica eluting with methylene dichloride did not separate the components. Recrystallisation from ether-light petroleum gave crystals, m.p. 85–90 °C, which were a mixture of (6) and (7),  $\lambda_{\text{max}}$  223 nm ( $\epsilon$  1 700);  $\nu_{\text{max}}$  3 620, 2 910, 1 680, 1 380, 1 200, and 900 cm<sup>-1</sup>;  $\delta_H$  1.61 (3 H, s), 1.68 (s), 1.8–2.2 (4 H, m), 2.5–2.9 (3 H, m), 4.9 (1 H, d), 5.3–5.5 (1 H, br d), and 6.72 (1 H, m). This mixture was carried forward to the next stage.

In the preparation of the deuteriated materials, the same procedure was followed, with replacement of sodium borohydride by sodium borodeuteride.

**Photocyclisation of Reduced Isoprene-Benzoquinone Diels-Alder Adduct.**—A solution of the reduced adducts (6) and (7) (0.84 g) in benzene (300 ml) was placed in the well of a standard photochemical apparatus. The solution was stirred and deoxygenated by nitrogen bubbling, and irradiated through quartz using a Hanovia medium-pressure mercury lamp. The reaction was conveniently monitored by g.l.c., being complete after 48 h. Evaporation of solvent yielded a clear viscous oil, shown by g.l.c. to contain a mixture of cyclised products in amounts corresponding to the composition of the starting material. Extensive chromatography on silica, eluting with a light petroleum-ether gradient, separated the isomers. The early fractions (0.17 g), after crystallisation from light petroleum, proved to be 5-hydroxy-9-methyltetracyclo[4.4.0.0<sup>3,8</sup>.0<sup>4,9</sup>]decan-5-one (1a), m.p. 101–102 °C (sublimes);  $\nu_{\text{max}}$  3 590, 2 930, 1 725, 1 210, 1 060, and 980 cm<sup>-1</sup>;  $\delta_H$  [<sup>2</sup>H<sub>6</sub>]benzene 0.94 (1 H, dt,  $J$  14 and 3.5 Hz), 1.07 (3 H, s), 1.23 (1 H, s), 1.52 (1 H, d,  $J$  12.5 Hz), 1.62 (1 H, d,  $J$  14.0 Hz), 1.77 (1 H, q,  $J$  12.5 and 3.0 Hz), 1.84 (1 H, q,  $J$  6.0 and 4.0 Hz), 1.96 (1 H, q,  $J$  9.2 and 2.0 Hz), 2.26 (1 H, m), 2.25 (2 H, m), and 3.83 (s, 1 H);  $m/z$  178 (17%), 132 (100), 117 (70), and 84 (63) (Found:  $M^+$ , 178.0994. C<sub>11</sub>H<sub>14</sub>O<sub>2</sub> requires  $M$ , 178.0993). The central fractions contained a mixture (0.32 g) and late fractions (0.22 g) were enriched in hydroxy-ketone (1b), isolated only as a 90% enriched mixture of isomers as a viscous oil,  $\nu_{\text{max}}$  3 570, 2 905, 1 710, 1 040, and 970 cm<sup>-1</sup>;  $\delta_H$  1.0 (1 H, dd,  $J$  12 and 3 Hz), 1.2 (3 H, s), 1.85 (2 H, m), 2.0 (1 H, dd,  $J$  12 and 3 Hz), 2.15 (1 H, d,  $J$  9 Hz), 2.3 (2 H, m), 2.45 (1 H, m), 2.70 (2 H, m), and 4.0 (1 H, s).

Similar photocyclisation of the deuteriated materials yielded hydroxy-ketone (1a; R = D) (Found: C, 73.9; H, 8.2%;  $M^+$ , 179.1058. C<sub>11</sub>H<sub>13</sub>DO<sub>2</sub> requires C, 73.7; H, 8.4%;  $M$ , 179.1057).

**Reduction of the Piperylene-Benzoquinone Adduct (8).**—A solution of the adduct<sup>14</sup> (8) (0.5 g) in 99% aqueous methanol (100 ml) was stirred and cooled at –20 °C under nitrogen. Sodium borohydride (0.02 g, 1.1 equiv.) was then added in portions and the mixture allowed to warm to room temperature. Monitoring by t.l.c. indicated complete reaction after ca. 1 h, and glacial acetic acid (0.1 ml) was added before removal of most solvent under reduced pressure. The residue was taken up

in ether (50 ml) which was washed with saturated aqueous sodium hydrogen carbonate and water before evaporation to an oil. Aqueous tetrahydrofuran (10 ml) and solid sodium fluoride (0.020 g) were then added and the homogenous mixture allowed to stand at room temperature for 2 h. Ether (50 ml) was then added, and solution was shaken with water (2.20 ml) before drying ( $\text{MgSO}_4$ ) and evaporation to yield an oil containing, by g.l.c., a single major component, (**9**;  $\text{R} = \text{H}$ ), finally purified, by chromatography on silica eluting with ether–light petroleum (0.23 g, 67%),  $\lambda_{\text{max}}$ , 224 nm ( $\epsilon$  3 400);  $\nu_{\text{max}}$ , 1 680, 1 375, 1 255, 1 070, 985, and 710  $\text{cm}^{-1}$ ; n.m.r. spectrum was temperature dependent (a conformational equilibration) and the high-temperature limit data are presented,  $\delta_{\text{H}}$  1.09 (3 H, m), 2.0–2.95 (6 H, unresolved), 4.6 (1 H, br, s), 5.65 (2 H, s), 5.93 (1 H, d,  $J$  4.5 Hz), and 6.83 (1 H, dd,  $J$  7.0 and 4.3 Hz);  $m/z$  178 (7%), 145 (43), 132 (100), 117 (84), and 84 (81) (Found: C, 74.1; H, 8.0%;  $M^+$ , 178.1003.  $\text{C}_{11}\text{H}_{14}\text{O}_2$  requires C, 74.2; H, 7.9%;  $M$ , 178.0994). Similar reaction using sodium borodeuteride yielded the deuteriated compound (**9**;  $\text{R} = \text{D}$ ).

**Photocyclization of (9; R = H) and (9; R = D).**—The procedure described above for photocyclization of (**6**) and (**7**) was followed. Irradiation of (**9**;  $\text{R} = \text{H}$ ) (0.24 g) yielded, after solvent evaporation and chromatography on silica, (**2a**;  $\text{R} = \text{H}$ ) (0.21 g). Recrystallization from ether–light petroleum gave crystals, m.p. 85–87 °C;  $\nu_{\text{max}}$ , 3 610, 1 740, 1 235, 1 070, and 970  $\text{cm}^{-1}$ ;  $\delta_{\text{H}}$  ( $[\text{}^2\text{H}_6]$ benzene) 0.86 (1 H, dt,  $J$  13 and 2.5 Hz) 1.17 (3 H, d,  $J$  7.5 Hz), 1.30 (1 H, brs, exchanges with  $\text{D}_2\text{O}$ ), 1.66 (1 H, d,  $J$  13 Hz), 2.0 (H, d,  $J$  8.5 Hz), 2.18 (3 H, m), 2.34 (1 H, m), 2.55 (2 H, m), and 4.00 (1 H, s);  $m/z$  (E.I.) 178 (22%), 133 (31), 121 (31), 117 (32), 110 (69), and 93 (100) (Found: C, 74.0; H, 8.1%;  $M^+$ , 178.0992.  $\text{C}_{11}\text{H}_{14}\text{O}_2$  requires C 74.2; H, 7.9%;  $M$ , 178.0994).

The deuteriated compound (**2a**;  $\text{R} = \text{D}$ ) prepared similarly from (**9**;  $\text{R} = \text{D}$ ) showed a weak band,  $\nu_{\text{max}}$ , 2 203  $\text{cm}^{-1}$ , in its i.r. spectrum and absence of  $\delta$  4.0 (s) in its n.m.r. spectrum (Found: C, 74.0; H, 8.1%;  $M^+$ , 179.1055.  $\text{C}_{11}\text{H}_{13}\text{DO}_2$  requires C, 73.7; H, 8.4%;  $M$ , 179.1057). Mass spectral analysis of TMS ethers gave a deuterium content of 86% [ $^2\text{H}_1$ ] for (**9a**;  $\text{R} = \text{D}$ ).

**Measurement of Kinetic Isotope Effects for Equilibrations of (1a and b) and of (2a and b).**—For the reactions of (**1a**), fluorenol was added as internal reference; for those of (**2a**), heptane-1,7-diol. The reference compound (0.5 mg) was weighed into each of two vials fitted with serum caps. The hydroxy-ketone (**1a**) or (**2a**), and the isotopomer (**1a**;  $\text{R} = \text{D}$ ) or (**2a**;  $\text{R} = \text{D}$ ) were then weighed separately (0.5 mg each) into the vials, which were then suspended in a thermostatted water-bath. Buffer solution (0.25 ml), which had been equilibrated to the same temperature, was added to each vial which was shaken for 30 s to dissolve the hydroxy-ketones before returning to the thermostatted bath and starting the stopwatch. At intervals, portions (0.002 ml) were removed from each vial by syringe. In the case of (**1a**) these were injected into smaller serum-capped vials containing redistilled trifluoroacetic anhydride (0.02 ml) and dry benzene (0.02 ml). In the case of (**2a**) they were injected into smaller serum-capped vials containing bis(trimethylsilyl)trifluoroacetamide with 1% trimethylchlorosilane. Between 15 and 20 samples were taken over three half-lives. When sampling was complete, the contents of each vial were analysed by capillary g.l.c. The mole-fraction of hydroxy-ketone was then calculated and rate constants calculated as described in the text. At the end of the experiment, the deuteriated material was isolated from the reaction by extraction and its deuterium content redetermined by mass spectrometry. Neither residual reactant nor product showed any loss of deuterium. Buffers used were sodium hydroxide–3,5-dimethylphenol (pH 11.31 and 12.32) or sodium hydroxide–trifluoroethanol (pH 12.94 and 13.70) in 1:1

v/v aqueous dioxane. Unbuffered sodium hydroxide solution was also used (pH 14.13). Ionic strengths were maintained at 0.5M by sodium chloride.

**Rates and Kinetic Isotope Effects for Rearrangements of (3; R = H or D).**—The preparations of [ $^2\text{H}_6$ ]dimethylsodium solutions, and of the n.m.r. samples of the alkoxides of these hydroxy-ketones, have already been described.<sup>16</sup> These methods were again used in the preparation of the mixture of isotopomers. In the preparation of a typical mixture, (**3**;  $\text{R} = \text{H}$ ) (0.0433 g) and (**3**;  $\text{R} = \text{D}$ ) (0.0415 g) were placed in a small, round-bottom flask. The solid mixture was then dissolved in ether and the ether then evaporated to yield an intimate mixture, which was freed of solvent by pumping at room temperature overnight. Deuterium content was determined by mass spectroscopy. The n.m.r. sample was then prepared using the mixture (0.12 g) and rates determined as described before. Mass spectral examination of the recovered material from the experiment showed no change in deuterium content.

**Deuteriation of Acetophenone.**—Acetophenone (5 g, 0.042 mol), deuterium oxide (15 ml), dioxane (15 ml), and potassium carbonate were refluxed together under a guard tube containing potassium hydroxide pellets for 48 h. The mixture was cooled, and light petroleum (50 ml) and water (100 ml) added. The layers were separated, and the organic layer washed with water before drying ( $\text{MgSO}_4$ ). Distillation yielded trideuterioacetophenone (4.65 g, 93%), b.p. 53–57 °C at 14 mmHg. Integration of signals at  $\delta$  2.2 and in the aromatic region showed the material was over 90% [ $^2\text{H}_3$ ]acetophenone.

**Oxidation of [ $^2\text{H}_3$ ]Acetophenone.**—The method of Riley and Gray<sup>32</sup> was adapted. Dioxane (25 ml), selenium dioxide (4.63 g, 0.042 mol), and deuterium oxide (0.83 ml) were placed in a flask fitted for reflux and carrying a guard tube containing potassium hydroxide. The mixture was heated and stirred until homogenous, then the deuteriated acetophenone was added in a single portion. The mixture was refluxed, and conversion monitored by h.p.l.c. When conversion was complete (ca. 66 h), the cooled mixture was filtered, and most water and dioxane removed by distillation. The residue was extracted with ether (100 ml), and the extracts washed quickly with saturated sodium hydrogen carbonate solution before drying ( $\text{MgSO}_4$ ) and evaporation. Bulb-to-bulb distillation yielded phenylglyoxal (3.01 g, 60%) as a pale yellow oil, b.p., 75–80 °C at 14 mmHg;  $\nu_{\text{max}}$ , 2 923, 1 696, 1 597, 1 450, 1 149, 1 085, 653, 711, and 685  $\text{cm}^{-1}$ ;  $\delta_{\text{H}}$  7.2–8.3 (5 H, m) and 10.3 (1 H, s). The oil was dissolved in 3–4 volumes of hot water and on cooling crystalline phenylglyoxal hydrate was formed (2.84 g). Recrystallisation from acetone–methylene dichloride gave crystals, m.p. 76–78 °C (lit., 74–76 °C),  $\nu_{\text{max}}$ , 3 348, 2 920, 1 697, 1 595, 1 449, 1 085, 952, 712, and 685  $\text{cm}^{-1}$ ;  $\delta_{\text{H}}$  ( $[\text{}^2\text{H}_6]$ acetone) 5.5 (removed by addition of  $\text{D}_2\text{O}$ , 1 H, s), 7.3–7.7 (3 H, m), and 7.9–8.3 (2 H, m);  $m/z$  (E.I.) 106 (13%), 105 (100), 77 (71), and 51 (17) (Found: C, 62.9; H, 5.2. Calc. for  $\text{C}_8\text{H}_8\text{O}_3$ : C, 62.8; H, 5.2%). Analysis of the ammonia CI mass spectrum comparing ratios of the  $M + 18$  peaks gave a deuterium content of 94.5%  $^2\text{H}_1$ .

**Rates and Kinetic Isotope Effects for Rearrangement of Phenylglyoxal Hydrate.**—A typical experiment is described. Saturated aqueous solutions of phenylglyoxal hydrate and the deuteriated material were prepared. Buffer solution (2.5 ml) was pipetted into each of three 1 cm stoppered quartz u.v. cells. These were then placed in the cell compartment of the u.v. spectrophotometer, one in the reference beam, and two in the thermostatted block of the automatic cell changer in the active beam. The cells were allowed to equilibrate to ambient temperature, then using microsyringes, 5  $\mu\text{l}$  of each of the



saturated solutions were added separately to the active cells. PGH shows  $\lambda_{\text{max}}$  250 nm ( $\log \epsilon$  4.06) and these solutions were ca.  $10^{-4}\text{M}$  in the glyoxal and showed absorbances ca. 1 immediately after mixing. Changes in absorbance at this wavelength were monitored automatically, voltages from the spectrometer being fed to the A/D converter of a BBC micro which timed and stored the data. At least 40 points were taken over three half-lives and rates were extracted from the data non-linear least-squares regression of exponential decay to data.<sup>33</sup>

The buffer solutions were borax (pH 9–10.5) and sodium phosphate (pH 10.5–12) with the ionic strength maintained at 0.1M.

### Acknowledgements

We thank S.E.R.C. for support of this work, and the Royal Society for a grant to C. I. F. W. for equipment.

### References

- 1 H. Sund, 'Pyridine Nucleotide Dependent Dehydrogenases,' W. de Gruyter, Berlin, 1977.
- 2 G. M. Kramer, in 'Industrial and Laboratory Alkylation,' eds. L. F. Albright and A. R. Gold, Am. Chem. Soc. Symposium 55, Washington, 1977, ch. 1.
- 3 L. Melander and W. H. Saunders, 'Reaction Rates of Isotopic Molecules,' Wiley, New York, 1980.
- 4 L. B. Sims and D. E. Lewis, in 'Isotopes in Organic Chemistry,' eds. E. Bunel and C. C. Lee, Elsevier, 1984, vol. 6.
- 5 B. G. Hutley, A. E. Mountain, I. H. Williams, G. M. Maggiora, and R. L. Schowen, *J. Chem. Soc., Chem. Commun.*, 1986, 267, 1303.
- 6 C. G. Swain, A. L. Powell, T. J. Lynch, S. R. Alpha, and R. Dunlap, *J. Am. Chem. Soc.*, 1979, **101**, 3584.
- 7 R. Stewart and T. W. Toone, *J. Chem. Soc., Perkin Trans. 2*, 1978, 1243.
- 8 J. E. C. Hutchins, D. A. Binder, and M. Kreevoy, *Tetrahedron*, 1986, **42**, 993.
- 9 P. Huszthy, K. Lempert, G. Simez, and J. Tamas, *J. Chem. Soc., Perkin Trans. 2*, 1982, 1671.
- 10 (a) J. C. Sheldon, J. H. Bowie, and R. N. Hayes, *Nouv. J. Chim.*, 1984, **8**, 79; (b) J. C. Sheldon, G. J. Currie, J. Lahnstein, R. N. Hayes, and J. H. Bowie, *ibid.*, 1985, **9**, 205.
- 11 G.-A. Craze and I. Watt, *J. Chem. Soc., Perkin Trans. 2*, 1981, 175.
- 12 W. K. Appel, T. J. Greenhaugh, J. R. Scheffer, J. Trotter, and L. Walsh, *J. Am. Chem. Soc.*, 1981, **102**, 1637.
- 13 A. M. Davis, M. I. Page, S. C. Mason, and I. Watt, *J. Chem. Soc., Chem. Commun.*, 1984, 1671.
- 14 W. J. Hehre, D. J. Defrees, M. Taagapera, B. A. Levi, S. K. Pollack, K. D. Summerhays, R. W. Taft, and M. Wolfsberg, *J. Am. Chem. Soc.*, 1979, **101**, 5532.
- 15 (a) D. A. Evans, J. M. Hoffman, and K. Truesdale, *J. Am. Chem. Soc.*, 1973, **95**, 5823; (b) D. Liotta, M. Sundame, and G. Barnum, *ibid.*, 1981, **103**, 3224.
- 16 I. Watt, S. N. Whittleton, and S. M. Whitworth, *Tetrahedron*, 1986, **42**, 1047.
- 17 J. Sandstrom, 'Dynamic NMR Spectroscopy,' Academic Press, London, 1982, pp. 25–29.
- 18 C. Daniel and F. S. Wood, 'Fitting Equations to Data,' Wiley-Interscience, New York, 1971.
- 19 W. v. E. Doering, T. I. Taylor, and E. F. Schoenwaldt, *J. Am. Chem. Soc.*, 1948, **70**, 455.
- 20 J. F. Hine and G. F. Koser, *J. Org. Chem.*, 1971, **36**, 3591.
- 21 D. D. Perrin, 'Ionization Constants of Inorganic Acids and Bases in Aqueous Solution,' Pergamon, Oxford, 1982 (IUPAC Chem. Data Series, 29).
- 22 D. J. Vander Jagt and L. P. B. Han, *Biochemistry*, 1973, **12**, 5161.
- 23 W. J. Hehre, R. F. Stewart, and J. A. Pople, *J. Chem. Phys.*, 1969, **51**, 2657; J. S. Binkley, J. A. Pople, and W. J. Hehre, *J. Am. Chem. Soc.*, 1980, **102**, 939; W. J. Hehre, R. Ditchfield, and J. A. Pople, *J. Chem. Phys.*, 1972, **56**, 2257; P. C. Hariharan and J. A. Pople, *Theor. Chim. Acta*, 1973, **28**, 213.
- 24 R. Ahlrichs and P. R. Taylor, *J. Chim. Phys.*, 1981, **78**, 315.
- 25 M. F. Guest and J. Kendrick, GAMESS User Manual CCP1/86/1, Daresbury Laboratory.
- 26 R. D. Amos, CADPAC User Manual CCP1/84/1, Daresbury Laboratory.
- 27 D. Moncrieff and V. R. Saunders, ATMOL Manual, NAT 648, University of Manchester Regional Computer Centre, 1986.
- 28 R. P. Bell, 'The Tunnel Effect in Chemistry,' Chapman and Hall, London, 1980.
- 29 J. L. Duncan and P. D. Mallinson, *Chem. Phys. Lett.*, 1973, **23**, 597; J. H. Taylor, W. S. Benedict, and J. Strong, *J. Chem. Phys.*, 1952, **20**, 1884.
- 30 Y.-D. Wu and K. N. Houk, *J. Am. Chem. Soc.*, 1987, **109**, 906.
- 31 D. D. Perrin, W. L. F. Armarego, and D. R. Perrin, 'Purification of Laboratory Chemicals,' Pergamon, 1983, 2nd edn.
- 32 (a) H. A. Riley and A. R. Gray, *Org. Synth.*, 1973, coll. vol. 5, p. 937; (b) H. V. Euler, H. Hasselquist, and A. Glaser, *Ark. Kemi*, 1951, **49**, 3.
- 33 J. K. Johnson, 'Numerical Methods in Chemistry,' Dekker, New York, 1980, p. 134.

Received 25th August 1987; Paper 7/1557